



Bis(2-methylpyridinium) tetrachloridocuprate(II): synthesis, structure and Hirshfeld surface analysis

Tahir Mehmood, Rajesh S. Bhosale* and J. Prakasha Reddy*

Department of Chemistry, School of Sciences, Indrashil University, Rajpur, Gujarat, 382740, India. *Correspondence e-mail: rajeshbhosale24@gmail.com, j.prakashareddy@gmail.com

Received 21 December 2020

Accepted 17 June 2021

Edited by G. Díaz de Delgado, Universidad de Los Andes, Venezuela

Keywords: 2-picoline complex; inorganic supramolecular chemistry; crystal structure; hydrogen bonding.

CCDC reference: 2090586

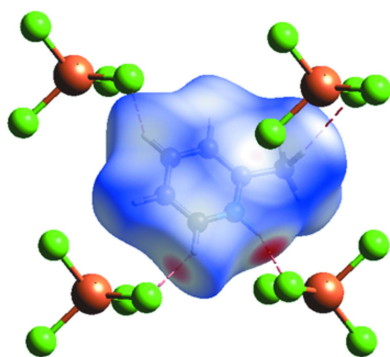
Supporting information: this article has supporting information at journals.iucr.org/e

The title compound, $(C_6H_8N)_2[CuCl_4]$, crystallizes in the monoclinic space group $I2/c$. The coordination around the copper atom is a distorted tetrahedron. The 2-methylpyridinium ion ($C_6H_8N^+$) interacts with the tetrachlorocuprate anion through $N-H\cdots Cl$ and $C-H(\text{phenyl})\cdots Cl$ contacts, forming a hydrogen-bonded layer-like structure. The supramolecular structure is further stabilized by $C-H(\text{methyl})\cdots Cl$ interactions between the layers.

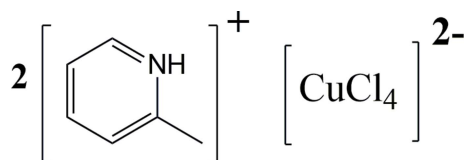
1. Chemical context

Supramolecular organic and inorganic chemistry have been studied both from the fundamental as well as the application point of view, which is evident from the literature (Ziach *et al.*, 2018; Thorat *et al.*, 2013; Burslem *et al.*, 2016). With the surge in the number of compounds reported, potential applications of supramolecular inorganic materials in energy storage, separation, catalysis, sensors, molecular magnets, optoelectronic materials, *etc.*, have attracted greater attention in recent years (Mueller *et al.*, 2006; Wan *et al.*, 2006; Férey *et al.*, 2003; James, 2003; Eddaoudi *et al.*, 2002; Ruben *et al.*, 2005; Kitagawa *et al.*, 2004; Stavila *et al.*, 2014). Because of the divergent combination of ligands and metal salts, an enormous number of structural architectures with different sizes and shapes could be constructed (Moulton & Zaworotko, 2001). The special characteristics and features such as ease of synthesis of the material, geometrically well-defined structures, exceptional tunability, post-synthetic modification, along with robustness of the material resulting from strong directional bonding, produce new opportunities and offer a unique platform amenable to the synthesis of more and more functional solids. For example, Adams *et al.* (2005) reported the synthesis of coordination compounds using a new synthetic route involving a thermal dehydrochlorination reaction in crystals of a pyridinium chlorometallate bicomponent system, *i.e.*, anionic metal complexes and organic cations.

As part of ongoing studies in our group (PrakashaReddy & Pedireddi, 2007; Reddy *et al.*, 2014), the synthesis of coordination complexes using pyridine ligands has been reported. Hence, we further extended our studies to utilize the pyridinium ligand and to study *in situ* the single-crystal-to-single-crystal transition (SCSCT) to investigate the reaction mechanism. In our endeavours to synthesize new functional solids, using a transition-metal anion and a pyridinium cation, we have chosen the $CuCl_2$ and 2-methylpyridinium salt complex. Herein, we report the synthesis and crystal structure



of a bis(2-methylpyridinium) tetrachlorocuprate coordination complex.



2. Structural commentary

The title complex crystallizes in the monoclinic space group $I2/c$. Since the Cu^{2+} cation occupies a special position, the asymmetric unit consists of a 2-methylpyridinium cation, $[2\text{-Me(Py)H}]^+$, and half of a tetrachlorocuprate(II) anion, $[\text{CuCl}_4]^{2-}$. The molecular structure of the complex along with the atom-labelling scheme is shown in Fig. 1. Each copper center is four-coordinated by chlorine anions and adopts a distorted tetrahedral geometry. Structural analysis shows that the $\text{Cl}-\text{Cu}-\text{Cl}$ angles vary from $98.55(2)$ to $137.4(3)^\circ$ with four angles smaller and two larger than the standard tetrahedral angle. A plausible reason for a larger deviation from the standard 109.5° might be due to the $\text{N}-\text{H}\cdots\text{Cl}$ and $\text{C}-\text{H}\cdots\text{Cl}$ interactions. A similar marked deviation from the standard tetrahedral angle has been previously observed by other research groups (Wyrzykowski *et al.*, 2011; Jasrotia *et al.*, 2018). The $\text{Cu}-\text{Cl}$ bond lengths [$\text{Cu1}-\text{Cl1} = 2.250(1)$ Å, $\text{Cu1}-\text{Cl2} = 2.249(1)$ Å] agree well with those reported for other structures (Marsh *et al.*, 1982; Dodds *et al.*, 2018; Molano *et al.*, 2020; Reddy, 2020). The intramolecular $\text{C}_{\text{ar}}-\text{C}_{\text{ar}}$ bond lengths in the $[2\text{-Me(Py)H}]^+$ fall in the range $1.370(3)$ – $1.395(3)$ Å. The $\text{N1}-\text{C2}$ and $\text{N1}-\text{C6}$ bond lengths are $1.350(2)$ and $1.346(2)$ Å, respectively.

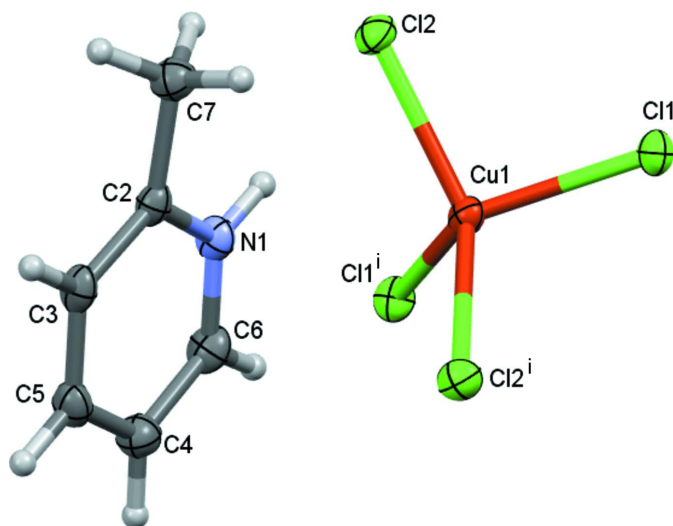


Figure 1

The molecular structure of the title compound, showing the atom labelling and displacement ellipsoids drawn at the 50% probability level. Hydrogen atoms are shown as small spheres of arbitrary size. [Symmetry code: (i) $1 - x, y, \frac{1}{2} - z$.]

Table 1

Hydrogen-bond geometry (Å, °).

$D-\text{H}\cdots A$	$D-\text{H}$	$\text{H}\cdots A$	$D\cdots A$	$D-\text{H}\cdots A$
$\text{N1}-\text{H1}\cdots\text{Cl1}^i$	0.88	2.93	3.4297 (16)	118
$\text{N1}-\text{H1}\cdots\text{Cl2}^i$	0.88	2.41	3.2050 (16)	150
$\text{C6}-\text{H6}\cdots\text{Cl1}^{ii}$	0.95	2.62	3.453 (2)	147
$\text{C7}-\text{H7A}\cdots\text{Cl2}$	0.98	2.92	3.850 (2)	159
$\text{C7}-\text{H7B}\cdots\text{Cl2}^{iii}$	0.98	2.98	3.872 (2)	151

Symmetry codes: (i) $-x + 1, -y, -z + 1$; (ii) $x + \frac{1}{2}, y - \frac{1}{2}, z + \frac{1}{2}$; (iii) $-x + 1, -y + 1, -z + 1$.

3. Supramolecular features and Hirshfeld surface analysis

In the crystal, complex molecules related by the twofold rotation axis are connected by pairs of $\text{N}-\text{H}\cdots\text{Cl}$ and $\text{C}_{\text{ar}}-\text{H}\cdots\text{Cl}$ interactions through a protonated N and an aromatic hydrogen attached to the carbon atom with the chloride ligand bonded to copper, forming a monomeric unit. These units interact with adjacent ones through $\text{C}_{\text{ar}}-\text{H}\cdots\text{Cl}$ hydrogen bonding (Table 1, Fig. 2). The $\text{N}-\text{H}\cdots\text{Cl}$ and $\text{C}-\text{H}\cdots\text{Cl}$ distances and associated bond angles lie within the ranges observed for other similar interactions reported in the literature (Adams *et al.*, 2005; Vittaya *et al.*, 2015; Wyrzykowski *et al.*

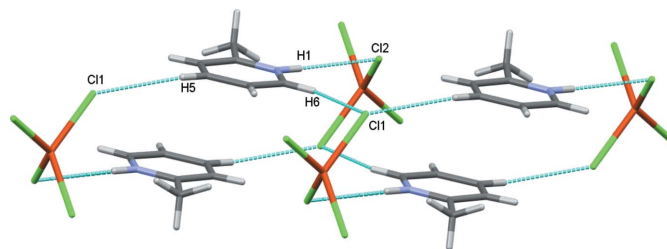


Figure 2

The $\text{N}-\text{H}\cdots\text{Cl}$ and $\text{C}-\text{H}\cdots\text{Cl}$ interactions between cations and anions in the crystal structure of the title compound.

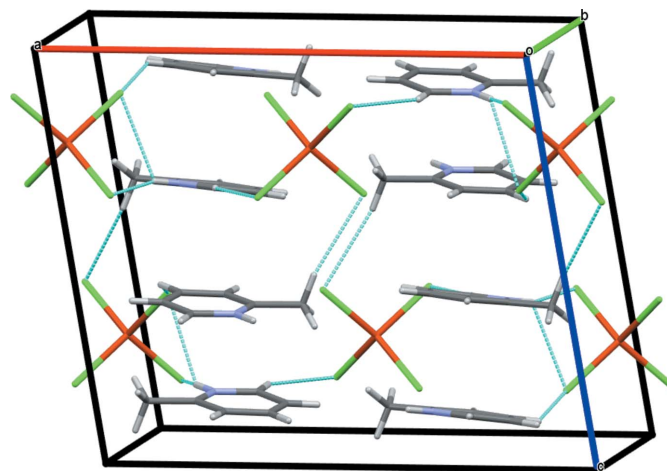


Figure 3

The crystal packing of the title compound viewed along the b axis with intermolecular contacts shown as dashed lines.

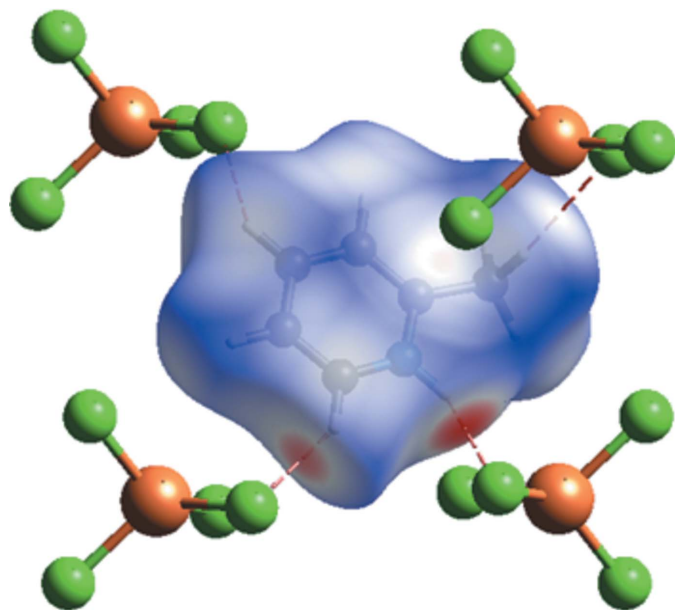


Figure 4
Hirshfeld surface mapped over d_{norm} highlighting the regions of N—H \cdots Cl and C—H \cdots Cl intermolecular contacts.

al., 2011; Jasrotia *et al.*, 2018). The supramolecular structure is further stabilized by C_{methyl}—H \cdots Cl interactions involving hydrogens of the methyl group and chlorides bonded to copper, generating layers along the crystallographic *b* axis (Fig. 3).

To further investigate the intermolecular interactions present in the title compound, a Hirshfeld surface analysis was performed and the two-dimensional fingerprint plots were generated with *Crystal Explorer17* (Turner *et al.*, 2017). The Hirshfeld surface mapped over d_{norm} and corresponding colours representing various interactions are shown in Fig. 4. The red points on the surface correspond to the N—H \cdots Cl and C—H \cdots Cl interactions. The two-dimensional fingerprint plots (McKinnon *et al.*, 2007) are shown in Fig. 5. On the Hirshfeld surface, the largest contribution (53.1%) comes from the weak van der Waals H \cdots H contacts. The interaction of d_{norm} on the two-dimensional fingerprint plot shows two spikes; each one corresponds to H \cdots H (39%) and H \cdots Cl/Cl \cdots H (32.5%) respectively. The H \cdots Cl interaction highlights the hydrogen bond between adjacent moieties in the crystal structure. The C \cdots H/H \cdots C (16.5%) interactions appear as two shoulders. These interactions play a crucial role in the overall stabilization of the crystal packing.

4. Database survey

A search of the Cambridge Structural Database (CSD, Version 5.41, update of August 2020; Groom *et al.*, 2016) revealed two related complexes containing 2-methylpyridinium: [2-methylpyridinium tetrachloroferrate(III)] (CCDC refcode WAYJEN; Wyrzykowski *et al.*, 2011) and [bis(2-methylpyridinium) tetrachloro-zinc(II)] (CCDC refcode WIPCUW; Jasrotia *et al.*, 2018). The molecular

structures of both WAYJEN and WIPCUW display three-dimensional supramolecular networks arising from N—H \cdots Cl and C—H \cdots Cl interactions. In addition, the search also revealed a 2-methylpyridine and copper chloride complex: [dichloro-bis(2-methylpyridine)Cu(II)] (CCDC refcode CMPYCU01; Marsh *et al.*, 1982) and [aqua-dichloro-bis(2-methylpyridine)Cu(II)] (CCDC refcode BIJWUM; Marsh *et al.*, 1982) and a very recently published dichloridomethanol-bis(2-methylpyridine)Cu(II) complex (Reddy, 2020). All of these structures display three-dimensional supramolecular networks stabilized by C—H \cdots Cl and O—H \cdots Cl interactions.

5. Synthesis and crystallization

Both 2-methylpyridine and anhydrous copper(II) chloride obtained from Aldrich were used for the reaction. Anhydrous copper(II) chloride (0.495 g, 0.005 mol) was dissolved in 10 ml of distilled water. To this solution, 2-methylpyridine (0.93 g, 0.01 mol) was added followed by addition of few drops of HCl (36%) and the resulting mixture was stirred for \sim 30 min. at room temperature. The solution was then allowed to stand at room temperature for a few hours before being filtered and left at room temperature for crystallization. Block-shaped, pale-yellow-coloured crystals were obtained after 36 h.

6. Refinement

Crystal data, data collection and structure refinement details are summarized in Table 2. H atoms were placed in calculated

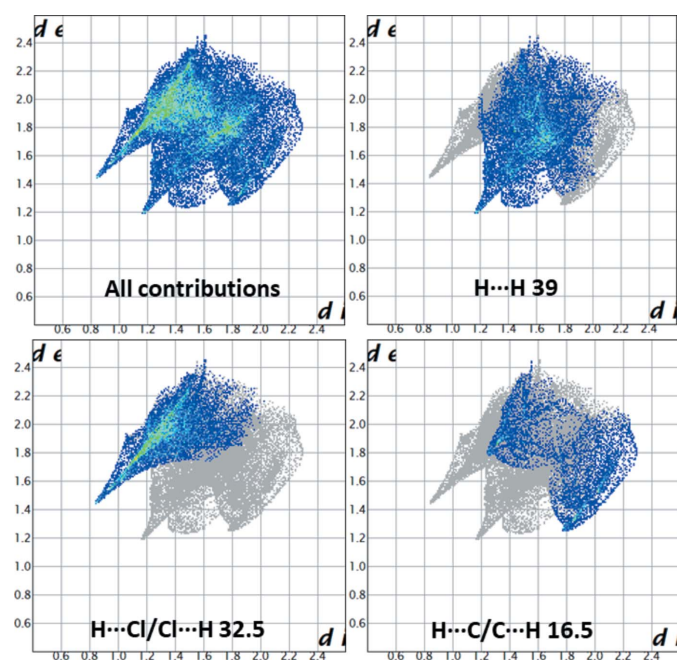


Figure 5
The full two-dimensional fingerprint plot for the organic cation in the title compound and those delineated into H \cdots H (39%), Cl \cdots H/H \cdots Cl (32.5%) and C \cdots H/H \cdots C (16.5%) contacts.

Table 2
Experimental details.

Crystal data	
Chemical formula	(C ₆ H ₈ N) ₂ [CuCl ₄]
<i>M_r</i>	393.62
Crystal system, space group	Monoclinic, <i>I2/c</i>
Temperature (K)	120
<i>a</i> , <i>b</i> , <i>c</i> (Å)	15.2354 (8), 8.3683 (3), 12.8372 (6)
β (°)	99.205 (5)
<i>V</i> (Å ³)	1615.60 (13)
<i>Z</i>	4
Radiation type	Mo <i>K</i> α
μ (mm ⁻¹)	2.00
Crystal size (mm)	0.32 × 0.27 × 0.25
Data collection	
Diffractometer	Agilent Xcalibur, Sapphire3
Absorption correction	Analytical (<i>CrysAlis PRO</i> ; Agilent, 2014)
<i>T_{min}</i> , <i>T_{max}</i>	0.848, 0.965
No. of measured, independent and observed [<i>I</i> > 2σ(<i>I</i>)] reflections	24556, 2821, 2324
<i>R_{int}</i>	0.071
(sin θ/λ) _{max} (Å ⁻¹)	0.758
Refinement	
<i>R</i> [<i>F</i> ² > 2σ(<i>F</i> ²)], <i>wR</i> (<i>F</i> ²), <i>S</i>	0.036, 0.081, 1.08
No. of reflections	2821
No. of parameters	88
H-atom treatment	H-atom parameters constrained
$\Delta\rho_{\max}$, $\Delta\rho_{\min}$ (e Å ⁻³)	0.58, -0.58

Computer programs: *CrysAlis PRO* (Agilent, 2014), *SUPERFLIP* (Palatinus & Chapuis, 2007; Palatinus & van der Lee, 2008; Palatinus *et al.*, 2012), *SHELXL* (Sheldrick, 2015) and *OLEX2* (Dolomanov *et al.*, 2009).

positions with C–H = 0.93–0.96 Å and N–H = 0.88 Å and refined as riding with fixed isotropic displacement parameters [*U*_{iso}(H) = 1.2–1.5*U*_{eq}(C, N)].

Acknowledgements

We thank Dr J. S. Yadav, Provost and Director (R&D) for his support and encouragement.

Funding information

Funding for this research was provided by: Indrashil University.

References

Adams, C. J., Crawford, P. C., Orpen, A. G., Podesta, T. J. & Salt, B. (2005). *Chem. Commun.* pp. 2457–2458.
 Agilent (2014). *CrysAlis PRO*. Agilent Technologies Ltd, Yarnton, England.
 Burslem, G. M., Kyle, H. F., Prabhakaran, P., Breeze, A. L., Edwards, T. A., Warriner, S. L., Nelson, A. & Wilson, A. J. (2016). *Org. Biomol. Chem.* **14**, 3782–3786.

Dodds, C. A. & Kennedy, A. R. (2018). *Acta Cryst.* **E74**, 1369–1372.
 Dolomanov, O. V., Bourhis, L. J., Gildea, R. J., Howard, J. A. K. & Puschmann, H. (2009). *J. Appl. Cryst.* **42**, 339–341.
 Eddaoudi, M., Kim, J., Rosi, N., Vodak, D., Wachter, J., O’Keeffe, M. & Yaghi, O. M. (2002). *Science*, **295**, 469–472.
 Férey, G., Latroche, M., Serre, C., Millange, F., Loiseau, T. & Percheron-Guégan, A. (2003). *Chem. Commun.* pp. 2976–2977.
 Groom, C. R., Bruno, I. J., Lightfoot, M. P. & Ward, S. C. (2016). *Acta Cryst.* **B72**, 171–179.
 James, S. L. (2003). *Chem. Soc. Rev.* **32**, 276–288.
 Jasrotia, D., Verma, S. K., Sridhar, B., Alvi, P. A. & Kumar, A. (2018). *Mater. Chem. Phys.* **207**, 98–104.
 Kitagawa, S., Kitaura, R. & Noro, S. I. (2004). *Angew. Chem. Int. Ed.* **43**, 2334–2375.
 Marsh, W. E., Hatfield, W. E. & Hodgson, D. J. (1982). *Inorg. Chem.* **21**, 2679–2684.
 McKinnon, J. J., Jayatilaka, D. & Spackman, M. A. (2007). *Chem. Commun.* pp. 3814–3816.
 Molano, M. F., Loret Velasquez, V. P., Erben, M. F., Nossa González, D. L., Loaiza, A. E., Echeverría, G. A., Piro, O. E., Tobón, Y. A., Ben Tayeb, K. & Gómez Castaño, J. A. (2020). *Acta Cryst.* **E76**, 148–154.
 Moulton, B. & Zaworotko, M. J. (2001). *Chem. Rev.* **101**, 1629–1658.
 Mueller, U., Schubert, M., Teich, F., Puetter, H., Schierle-Arndt, K. & Pastré, J. (2006). *J. Mater. Chem.* **16**, 626–636.
 Palatinus, L. & Chapuis, G. (2007). *J. Appl. Cryst.* **40**, 786–790.
 Palatinus, L., Prathapa, S. J. & van Smaalen, S. (2012). *J. Appl. Cryst.* **45**, 575–580.
 Palatinus, L. & van der Lee, A. (2008). *J. Appl. Cryst.* **41**, 975–984.
 PrakashaReddy, J. & Pedireddi, V. R. (2007). *Eur. J. Inorg. Chem.* pp. 1150–1158.
 Reddy, J. P. (2020). *Acta Cryst.* **E76**, 1771–1774.
 Reddy, J. P., Swain, D. & Pedireddi, V. R. (2014). *Cryst. Growth Des.* **14**, 5064–5071.
 Ruben, M., Ziener, U., Lehn, J. M., Ksenofontov, V., Gütllich, P. & Vaughan, G. B. M. (2005). *Chem. Eur. J.* **11**, 94–100.
 Sheldrick, G. M. (2015). *Acta Cryst.* **C71**, 3–8.
 Stavila, V., Talin, A. A. & Allendorf, M. D. (2014). *Chem. Soc. Rev.* **43**, 5994–6010.
 Thorat, V. H., Ingole, T. S., Vijayadas, K. N., Nair, R. V., Kale, S. S., Ramesh, V. V. E., Davis, H. C., Prabhakaran, P., Gonnade, R. G., Gawade, R. L., Puranik, V. G., Rajamohanam, P. R. & Sanjayan, G. J. (2013). *Eur. J. Org. Chem.* pp. 3529–3542.
 Turner, M. J., McKinnon, J. J., Wolff, S. K., Grimwood, D. J., Spackman, P. R., Jayatilaka, D. & Spackman, M. A. (2017). *CrystalExplorer17*. The University of Western Australia.
 Vittaya, L., Leesakul, N., Saithong, S. & Chainok, K. (2015). *Acta Cryst.* **E71**, m201–m202.
 Wan, Y., Yang, H. & Zhao, D. (2006). *Acc. Chem. Res.* **39**, 423–432.
 Wyrzykowski, D., Wera, M., Sikorski, A., Jacewicz, D. & Chmurnyński, L. (2011). *Cent. Eur. J. Chem.* **9**, 1096–1101.
 Ziach, K., Chollet, C., Parissi, V., Prabhakaran, P., Marchivie, M., Corvaglia, V., Bose, P. P., Laxmi-Reddy, K., Godde, F., Schmitter, J.-M., Chaignepain, S., Pourquier, P. & Huc, I. (2018). *Nat. Chem.* **10**, 511–518.

supporting information

Acta Cryst. (2021). E77, 726-729 [https://doi.org/10.1107/S2056989021006277]

Bis(2-methylpyridinium) tetrachloridocuprate(II): synthesis, structure and Hirshfeld surface analysis

Tahir Mehmood, Rajesh S. Bhosale and J. Prakasha Reddy

Computing details

Data collection: *CrysAlis PRO* (Agilent, 2014); cell refinement: *CrysAlis PRO* (Agilent, 2014); data reduction: *CrysAlis PRO* (Agilent, 2014); program(s) used to solve structure: Superflip (Palatinus & Chapuis, 2007; Palatinus & van der Lee, 2008; Palatinus *et al.*, 2012); program(s) used to refine structure: *SHELXL* (Sheldrick, 2015); molecular graphics: *OLEX2* (Dolomanov *et al.*, 2009); software used to prepare material for publication: *OLEX2* (Dolomanov *et al.*, 2009).

Bis(2-methylpyridinium) tetrachloridocuprate(II)

Crystal data

(C₆H₈N)₂[CuCl₄]
M_r = 393.62
 Monoclinic, *I*2/c
a = 15.2354 (8) Å
b = 8.3683 (3) Å
c = 12.8372 (6) Å
 β = 99.205 (5)°
V = 1615.60 (13) Å³
Z = 4

F(000) = 796
D_x = 1.618 Mg m⁻³
 Mo *K*α radiation, λ = 0.71073 Å
 Cell parameters from 5462 reflections
 θ = 2.9–32.5°
 μ = 2.00 mm⁻¹
T = 120 K
 Blocks, pale yellow
 0.32 × 0.27 × 0.25 mm

Data collection

Agilent Xcalibur, Sapphire3
 diffractometer
 Detector resolution: 16.1511 pixels mm⁻¹
 ω scans
 Absorption correction: analytical
 (CrysAlisPro; Agilent, 2014)
T_{min} = 0.848, *T_{max}* = 0.965
 24556 measured reflections

2821 independent reflections
 2324 reflections with *I* > 2σ(*I*)
R_{int} = 0.071
 θ_{\max} = 32.6°, θ_{\min} = 2.9°
h = -22→22
k = -11→12
l = -19→19

Refinement

Refinement on *F*²
 Least-squares matrix: full
R[*F*² > 2σ(*F*²)] = 0.036
wR(*F*²) = 0.081
S = 1.08
 2821 reflections
 88 parameters
 0 restraints
 Primary atom site location: iterative

Hydrogen site location: inferred from
 neighbouring sites
 H-atom parameters constrained
 $w = 1/[\sigma^2(F_o^2) + (0.0308P)^2 + 1.4147P]$
 where $P = (F_o^2 + 2F_c^2)/3$
 $(\Delta/\sigma)_{\max} < 0.001$
 $\Delta\rho_{\max} = 0.58 \text{ e } \text{Å}^{-3}$
 $\Delta\rho_{\min} = -0.58 \text{ e } \text{Å}^{-3}$

Special details

Geometry. All esds (except the esd in the dihedral angle between two l.s. planes) are estimated using the full covariance matrix. The cell esds are taken into account individually in the estimation of esds in distances, angles and torsion angles; correlations between esds in cell parameters are only used when they are defined by crystal symmetry. An approximate (isotropic) treatment of cell esds is used for estimating esds involving l.s. planes.

Fractional atomic coordinates and isotropic or equivalent isotropic displacement parameters (\AA^2)

	<i>x</i>	<i>y</i>	<i>z</i>	$U_{\text{iso}}^*/U_{\text{eq}}$
Cu1	0.500000	0.22261 (4)	0.250000	0.01825 (9)
Cl1	0.38953 (3)	0.10590 (5)	0.13863 (3)	0.02196 (11)
Cl2	0.41898 (3)	0.32033 (5)	0.36739 (4)	0.02260 (11)
N1	0.68501 (11)	0.01294 (19)	0.63521 (12)	0.0218 (3)
H1	0.642734	−0.054296	0.645210	0.026*
C2	0.66434 (12)	0.1697 (2)	0.62543 (13)	0.0197 (3)
C3	0.73176 (13)	0.2747 (2)	0.61076 (14)	0.0222 (4)
H3	0.720458	0.386273	0.605979	0.027*
C4	0.83354 (14)	0.0533 (2)	0.61276 (16)	0.0261 (4)
H4	0.890816	0.012622	0.607122	0.031*
C5	0.81548 (14)	0.2165 (2)	0.60311 (15)	0.0247 (4)
H5	0.861102	0.288380	0.591178	0.030*
C6	0.76632 (14)	−0.0468 (2)	0.63060 (15)	0.0254 (4)
H6	0.777088	−0.158092	0.639704	0.031*
C7	0.57039 (13)	0.2174 (2)	0.62851 (16)	0.0259 (4)
H7A	0.536395	0.214343	0.556960	0.039*
H7B	0.569141	0.325976	0.656845	0.039*
H7C	0.543936	0.143189	0.673767	0.039*

Atomic displacement parameters (\AA^2)

	U^{11}	U^{22}	U^{33}	U^{12}	U^{13}	U^{23}
Cu1	0.02142 (16)	0.01465 (15)	0.01929 (16)	0.000	0.00510 (12)	0.000
Cl1	0.0253 (2)	0.0174 (2)	0.0226 (2)	−0.00165 (16)	0.00223 (17)	−0.00185 (15)
Cl2	0.0276 (2)	0.0172 (2)	0.0246 (2)	0.00035 (16)	0.00935 (17)	−0.00340 (16)
N1	0.0268 (8)	0.0154 (7)	0.0235 (7)	−0.0023 (6)	0.0054 (6)	0.0011 (6)
C2	0.0264 (9)	0.0172 (8)	0.0155 (8)	−0.0004 (7)	0.0033 (7)	0.0000 (6)
C3	0.0311 (10)	0.0150 (8)	0.0203 (8)	−0.0030 (7)	0.0040 (7)	0.0004 (6)
C4	0.0251 (10)	0.0266 (10)	0.0267 (9)	0.0016 (8)	0.0040 (8)	−0.0010 (8)
C5	0.0281 (10)	0.0221 (9)	0.0244 (9)	−0.0069 (7)	0.0056 (8)	−0.0008 (7)
C6	0.0326 (10)	0.0172 (9)	0.0265 (10)	0.0031 (7)	0.0048 (8)	0.0016 (7)
C7	0.0263 (10)	0.0243 (10)	0.0276 (10)	0.0018 (7)	0.0061 (8)	0.0004 (8)

Geometric parameters (\AA , $^\circ$)

Cu1—Cl1 ⁱ	2.2496 (5)	C3—C5	1.383 (3)
Cu1—Cl1	2.2496 (5)	C4—H4	0.9500
Cu1—Cl2	2.2492 (4)	C4—C5	1.395 (3)
Cu1—Cl2 ⁱ	2.2492 (4)	C4—C6	1.370 (3)

N1—H1	0.8800	C5—H5	0.9500
N1—C2	1.350 (2)	C6—H6	0.9500
N1—C6	1.346 (2)	C7—H7A	0.9800
C2—C3	1.387 (3)	C7—H7B	0.9800
C2—C7	1.493 (3)	C7—H7C	0.9800
C3—H3	0.9500		
Cl1—Cu1—Cl1 ⁱ	128.54 (3)	C5—C4—H4	121.0
Cl2 ⁱ —Cu1—Cl1	99.614 (17)	C6—C4—H4	121.0
Cl2 ⁱ —Cu1—Cl1 ⁱ	98.550 (17)	C6—C4—C5	118.10 (19)
Cl2—Cu1—Cl1	98.549 (17)	C3—C5—C4	120.61 (18)
Cl2—Cu1—Cl1 ⁱ	99.616 (17)	C3—C5—H5	119.7
Cl2 ⁱ —Cu1—Cl2	137.36 (3)	C4—C5—H5	119.7
C2—N1—H1	118.0	N1—C6—C4	119.91 (18)
C6—N1—H1	118.0	N1—C6—H6	120.0
C6—N1—C2	124.00 (17)	C4—C6—H6	120.0
N1—C2—C3	117.46 (17)	C2—C7—H7A	109.5
N1—C2—C7	117.88 (17)	C2—C7—H7B	109.5
C3—C2—C7	124.64 (17)	C2—C7—H7C	109.5
C2—C3—H3	120.1	H7A—C7—H7B	109.5
C5—C3—C2	119.88 (17)	H7A—C7—H7C	109.5
C5—C3—H3	120.1	H7B—C7—H7C	109.5
N1—C2—C3—C5	2.2 (3)	C6—N1—C2—C3	-0.6 (3)
C2—N1—C6—C4	-1.5 (3)	C6—N1—C2—C7	177.92 (17)
C2—C3—C5—C4	-1.7 (3)	C6—C4—C5—C3	-0.4 (3)
C5—C4—C6—N1	2.0 (3)	C7—C2—C3—C5	-176.27 (18)

Symmetry code: (i) $-x+1, y, -z+1/2$.

Hydrogen-bond geometry (\AA , $^\circ$)

$D-H\cdots A$	$D-H$	$H\cdots A$	$D\cdots A$	$D-H\cdots A$
N1—H1 \cdots Cl1 ⁱⁱ	0.88	2.93	3.4297 (16)	118
N1—H1 \cdots Cl2 ⁱⁱ	0.88	2.41	3.2050 (16)	150
C6—H6 \cdots Cl1 ⁱⁱⁱ	0.95	2.62	3.453 (2)	147
C7—H7A \cdots Cl2	0.98	2.92	3.850 (2)	159
C7—H7B \cdots Cl2 ^{iv}	0.98	2.98	3.872 (2)	151

Symmetry codes: (ii) $-x+1, -y, -z+1$; (iii) $x+1/2, y-1/2, z+1/2$; (iv) $-x+1, -y+1, -z+1$.